Original Article

The Values of Wall Shear Stress, Turbulence Kinetic Energy and Blood Pressure Gradient are Associated with Atherosclerotic Plaque Erosion in Rabbits

Naoki Sameshima[1], Atsushi Yamashita[1], Shinya Sato[2], Shuntaro Matsuda[3], Yunosuke Matsuura[4] and Yujiro Asada[1]

[1]Department of Pathology, Faculty of Medicine, University of Miyazaki, Miyazaki, Japan
[2]Division of Pathology, University of Miyazaki Hospital, University of Miyazaki, Miyazaki, Japan
[3]Divisions of Community and Family Medicine, Faculty of Medicine, University of Miyazaki, Miyazaki, Japan
[4]Department of Internal Medicine, Faculty of Medicine, University of Miyazaki, Miyazaki, Japan

***Aim*: To clarify the contribution of hemodynamic factors to the onset of plaque erosion in smooth muscle cell (SMC)-rich atherosclerotic plaque.**
***Methods*: We developed a rabbit model of SMC-rich atherosclerotic plaque with various degree of stenosis induced by incomplete ligation and generated three-dimensional models of five rabbit femoral arteries based on 130-162 serial histological cross-sections at 100-μm intervals per artery. We performed a computational blood flow simulation using the Reynolds-averaged Navier-Stokes model and calculated the wall shear stress (WSS), turbulence kinetic energy (TKE), blood pressure (BP) and blood pressure gradients (BPG) in eight sections (the inlet, the stenotic portion and areas 1, 2 and 5 mm from the stenotic portion) in each rabbit. We also investigated whether the magnitude of WSS or TKE was related to the presence or absence of erosive injury by evaluating six points (the locally highest, median and lowest of WSS or TKE) in each section.**
***Results*: The magnitudes of WSS, TKE and BPG, but not BP, correlated significantly with the extent of histologically-defined plaque erosion (WSS, $r=0.55$, $p<0.001$; TKE, $r=0.53$, $p<0.001$; BPG, $r=0.61$, $p<0.0001$, $n=40$). The values for WSS and TKE were significantly larger at sites with, compared to without, erosive injury ($n=107$ and $n=119$ points, respectively; both $p<0.0001$).**
***Conclusions*: These results suggest that increased values of WSS, TKE and BPG considerably contribute to the onset of plaque erosion.**

J Atheroscler Thromb, 2014; 21:831-838.

Key words: Plaque erosion, Animal model, Computational fluid dynamics

Introduction

Acute cardiovascular events are triggered by the disruption of coronary atherosclerotic plaques, involving rupture and erosion[1, 2]. Rupture is more likely to occur in plaques with a large lipid core encapsulated by a thin fibrous cap containing inflammatory cell infiltration[1-3]. Accumulating evidence supports the notion that inflammation and matrix degradation play crucial roles in the pathogenesis of plaque rupture. On the other hand, plaque erosion is characterized by superficial plaque injury. The morphological characteristics include an abundance of smooth muscle cells (SMCs) and extracellular matrix, whereas the lipid core is small or absent and inflammatory cells are scant[1, 2, 4]. Plaque erosion accounts for 20% to 40% of coronary sudden deaths and is particularly common among patients <50 years of age and smokers, with the frequency being higher in women[4-7]. These histological and clinical differences indicate that the underlying mechanisms of plaque erosion differ from those of plaque rupture. However, the details of the mecha-

Address for correspondence: Yujiro Asada, Department of Pathology, Faculty of Medicine, University of Miyazaki, 5200 Kihara, Kiyotake, Miyazaki 889-1692, Japan
E-mail: yasada@med.miyazaki-u.ac.jp
Received: December 9, 2013
Accepted for publication: February 14, 2014

nisms underlying the development of plaque erosion remain unclear[1, 2].

Blood flow-induced mechanical stress is an essential factor in the development of atherosclerosis and thrombosis. Various mechanical factors likely also play a role in plaque rupture, including wall shear stress (WSS), blood pressure (BP) and the tensile stress concentration within the lesion wall[8-11]. Endothelial cells preferentially become damaged downstream of atherosclerotic plaques, where the blood flow is disturbed and shear stress is lower than at upstream portions[12]. Experimental acute arterial stenosis has been shown to induce endothelial changes or damage of the normal aorta as well as coronary and carotid arteries[13, 14]. We recently demonstrated that the blood flow disturbed by acute vascular narrowing induces superficial erosive injury to SMC-rich plaque with consequent thrombus formation[15]. Therefore, hemodynamic forces, such as a disturbed or turbulent blood flow induced by stenosis or vasoconstriction in particular, are crucial factors in generating erosive injury. However, how blood flow-induced mechanical factors contribute to the onset of plaque erosion remains unclear.

We assessed WSS, turbulence kinetic energy (TKE), BP and blood pressure gradient (BPG) values in a rabbit model of plaque erosion and computational fluid dynamics in order to determine the contribution of blood flow-induced mechanical factors to the onset of plaque erosion.

Methods

Ethics Statement

The Animal Care Committee of Miyazaki University approved the animal research protocols (permit number 2010-511), which conformed to the Guide for the Care and Use of Laboratory Animals published by the US National Institutes of Health. All efforts were made to minimize suffering.

Generation of a Rabbit Model of Plaque Erosion

Five male Japanese white rabbits weighing 2.5 to 3.0 kg were fed a conventional diet. Surgery proceeded under aseptic conditions and general anesthesia with the administration of intravenous pentobarbital (25 mg/kg). An angioplasty balloon catheter (diameter, 2.5 mm; length, 9 mm; QUANTUM, Boston Scientific, Galway, Ireland) was inserted via the carotid artery into the right femoral artery under fluoroscopic guidance. The catheter was inflated to 1.5 atm and retracted three times to induce SMC-rich atherosclerotic plaque formation in the right femoral artery[15]. Three weeks later, a 21-G needle (1 cm in length) was longitudinally placed along the ventral surface of the injured femoral artery, and a 1-0 silk suture was tied at one point around both the artery and the needle, which was then removed to resume the blood flow[16]. The blood flow was reduced to approximately 25% of the initial level measured using a T106 transit flow meter (Transonic Systems Inc., NY, USA). These techniques were carried out under the utmost care in order to prevent traumatic endothelial injury. One hour later, the rabbits were injected with heparin (500 U/kg, i.v.) and sacrificed with an overdose of pentobarbital (60 mg/kg, i.v.). The animals were then perfused with 0.01 mol/L of phosphate buffered saline and 50 mL of 4% paraformaldehyde for the histological analyses.

Histological Sections and Vascular Geometry Reconstruction

The excised femoral arteries were fixed in 4% paraformaldehyde for 12 hours at 4℃ and longitudinally embedded in paraffin. Sections (3 μm thick) obtained at 100-μm intervals were stained with hematoxylin and eosin. Histological arterial sections (130 to 162 slices per artery) were captured as digital images in JPEG format with a resolution of 640×480 pixels using the NIS-Element D3.2 microscope imaging software program (Nikon Instruments, Tokyo, Japan). The image files were then aligned using the Avizo 6.1 image processing software program (FEI Visualization Sciences Group, Oregon, USA) in order to reconstruct the 3-dimensional (3D) geometry (**Fig. 1A**). Unreasonable excess bumps between slices were manually smoothed. Aligned images of the arterial walls were processed via surface rendering, and the extracted inner vascular cavities were saved into 3D computer-aided design data in the STereoLithography (STL) format.

Analysis of Computational Fluid Dynamics (CFD)

Vascular geometrical STL files were applied to a CFD analysis using the OpenFOAM® 2.0 open source CFD toolbox (OpenCFD Ltd./OpenFOAM foundation, Bracknell, UK) under the following conditions. Blood was assumed to be a non-compressive Newtonian fluid. The blood flow at the inlet was set as a continuous flow with a plugged velocity profile of $|\boldsymbol{u}_{\text{mean, inlet}}| = 12.7$ cm/s in the axial direction determined based on a flow reduction model[17]. The blood properties were selected according to the literature as follows: dynamic viscosity $\nu = 3.873 \times 10^{-6}$ m^2/s and density $\rho = 1044$ kg/m^3 [18, 19]. These values are valid under physiological conditions, and the vascular wall was assumed to be rigid.

The effects of turbulence were evaluated in the

Reynolds-averaged Navier-Stokes (RANS) model. The initial TKE (k) in the inlet was given as:

$k = 1/2\ (\boldsymbol{u}_{mean,\ inlet} \times I)^2$, where I is the turbulent intensity. The values for, or distribution of, BP, fluid velocity, WSS and TKE did not differ significantly in a pilot study of turbulent conditions that were very low (I=0.00005) or became higher (I=0.05). Therefore, we established I=0.00005 as the initial inlet condition. The systems were developed by solving the Navier-Stokes equation using time steps.

$$\frac{\partial \boldsymbol{u}}{\partial t} + (\boldsymbol{u} \cdot \nabla)\boldsymbol{u} = -\frac{1}{\rho}\nabla p + \nu \nabla^2 \boldsymbol{u} \text{ (Navier-Stokes equation)}$$

$$\nabla \cdot \boldsymbol{u} = 0 \text{ (equation of continuity)}^{20)},$$

where $\boldsymbol{u}$ is the flow velocity, ρ is the density, p is BP and ν is the dynamic viscosity. The blood pressure gradient (BPG) was defined as the change ratio of the mean blood pressure per distance between two observed slices, practically calculated with a distance of 0.1 mm.

$$BPG = (BP_{mean,\ sliceX} - BP_{mean,\ sliceX+\Delta X})/\Delta X\ (\Delta X = 0.1\ mm)$$

All CFD simulations finished with a residual error of $< 10^{-5}$.

Data Analysis

We assessed the relationships between WSS, TKE, BP or BPG and the extent of erosive damage using 40 sections of longitudinal portions comprising the inlet, the most stenotic portion and areas 1, 2, 5 mm proximal or distal from the most stenotic portion of five arteries (**Fig. 1A**). Erosive injury was histologically defined as endothelial cell detachment with thrombus formation (**Fig. 1B**)[5, 15]. We measured the ratio of the length of erosive injury to the circumference in each histological section and expressed this figure as the erosion length/circumference (%) for each longitudinal portion. The WSS, TKE, relative BP to the outlet and BPG are expressed as mean values for the corresponding cross sections.

We examined whether the magnitudes of WSS and TKE correlated with the sites of erosive injury. Six points were selected from the circumference (the locally highest, median and lowest value of WSS and TKE) in each section, and the presence or absence of erosive injury was assessed point by point (**Fig. 4A**) across 226 points because 14 points overlapped with other points. Since the BPG was assessed between sections in our model, it was not evaluated in this point assessment.

Statistical Analysis

All data are presented as the mean and standard deviation or median with interquartile range. Relationships between factors were evaluated using Spearman's rank correlation test. Differences between groups were tested using the two-tailed Mann-Whitney *U*-test (JMP® 8.0.2, SAS Institute Inc., Cary, North Carolina, USA). A p value of < 0.05 was considered to be statistically significant.

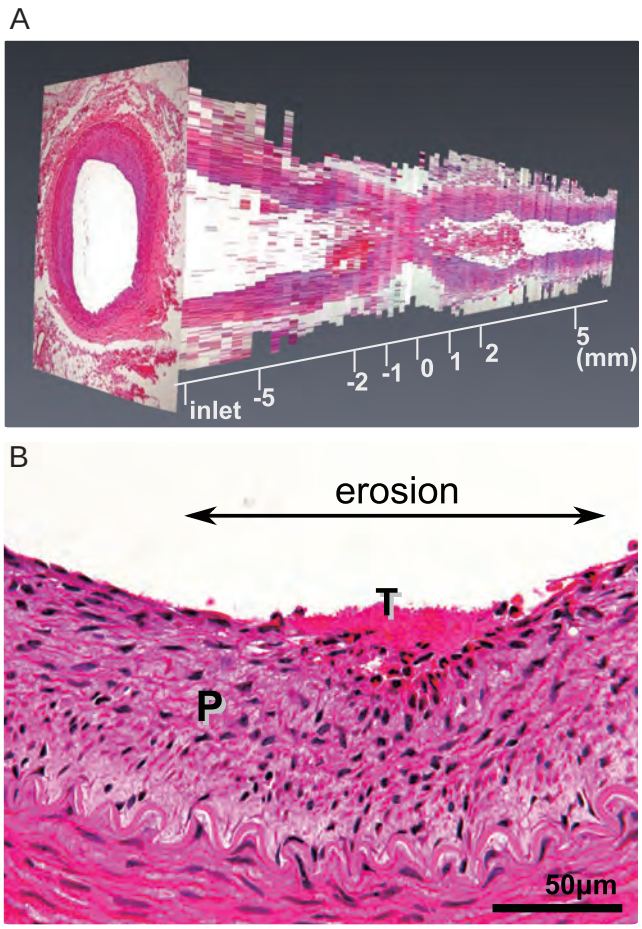

Fig. 1. Representative reconstructed image and microphotograph of a rabbit femoral artery with SMC-rich plaque.

A. Representative 3D-reconstruction image of the rabbit femoral artery. A thrombus has formed around the stenotic portion.
B. Microphotograph highlights the surface portion of SMC-rich plaque (P) with erosive injury (arrow) and thrombus formation (T). Balloon injury has induced atherosclerotic plaque-rich SMC in the rabbit femoral artery.

Results

WSS, TKE, BP and BPG in the Reconstructed Vessels

Fig. 2A-C shows the mean values for WSS, TKE and BP at the longitudinal distance from the most ste-

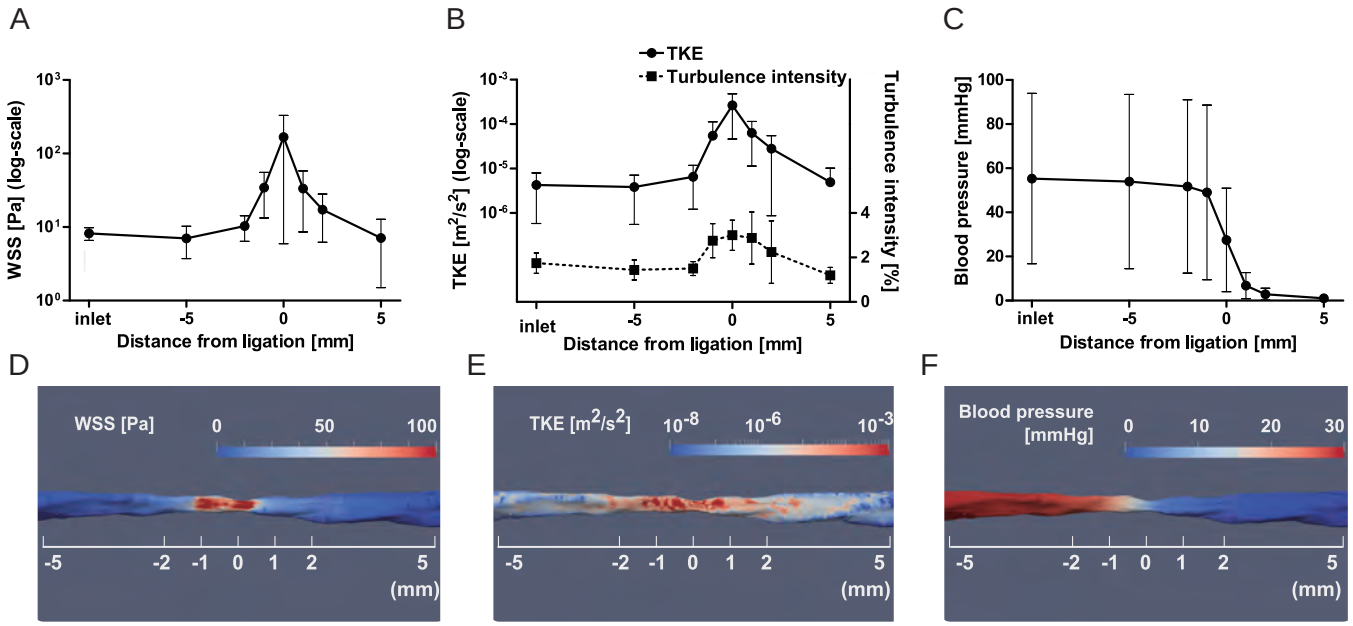

Fig. 2. Values for WSS, TKE and BP at a longitudinal distance from the stenotic portion.

Values for WSS (A), TKE and turbulent intensity (B) and BP (C) at a longitudinal distance from the stenotic portion ($n=5$ each). Blood pressure is shown relative to the outlet.

Representative 3D image of a reconstructed artery showing the distribution of WSS (D), TKE (E) and BP (F). The value of WSS is increased at the stenotic portion. The value of TKE is broadly increased in terms of the proximal, stenotic, distal and peak values observed at the stenotic portion. Blood pressure rapidly decreased across the stenotic portion.

notic portion. Blood pressure is expressed relative to the value at the outlet. The magnitudes of WSS and TKE peaked at the stenotic portion. The CFD simulation showed a rapid decrease in BP across the stenotic portion, indicating a high BPG. **Fig. 2D-F** demonstrates the distribution of WSS, TKE and BP from the 5 mm proximal portion to the 5 mm distal portion of the 3D-image of the reconstructed artery. The magnitude of the WSS increased at the stenotic portion. The magnitude of TKE broadly and heterogeneously increased in this model and peaked at the stenotic portion, whereas BP rapidly decreased across the stenotic portion.

Relationships between Erosive Injury and WSS, TKE and BPG

We measured the ratios of the length of erosive injury to the circumference in the histological sections in order to determine whether the extent of erosive injury was associated with the values of WSS, TKE, BP and BPG. Erosive injury was broadly distributed in the proximal, stenotic and distal portions (**Fig. 3A**), maximal at the stenotic portion and positively correlated with the WSS, TKE and BPG of the corresponding arterial sections (**Fig. 3B**, **C** and **D**), but not with BP (**Fig. 3E**).

WSS and TKE Values at the Erosive and Non-Erosive Points

We examined whether the magnitudes of WSS and of TKE correlated with the presence or absence of erosive injury. **Fig. 4A** and **B** shows representative cross sectional images 2 mm distal from the stenotic portion. Six points indicate the locally highest, median and lowest WSS and TKE values. The magnitudes of WSS and TKE were unevenly distributed with a relatively similar pattern. The sites of erosive injury were also unevenly distributed, although they tended to localize where the magnitudes of WSS and TKE were higher. As shown in **Fig. 4C** and **D**, the magnitudes of WSS and TKE were statistically higher at sites with, compared to without, erosive injury ($n=107$ and $n=119$ points, respectively; both $p<0.0001$) among 226 points per 40 sections.

Discussion

In this study, erosive injury of SMC-rich atherosclerotic plaque was found to be associated with a turbulent blood flow and increased WSS, TKE and BPG values in rabbits.

Plaque erosion is a type of atherosclerotic plaque disruption responsible for a relatively large proportion

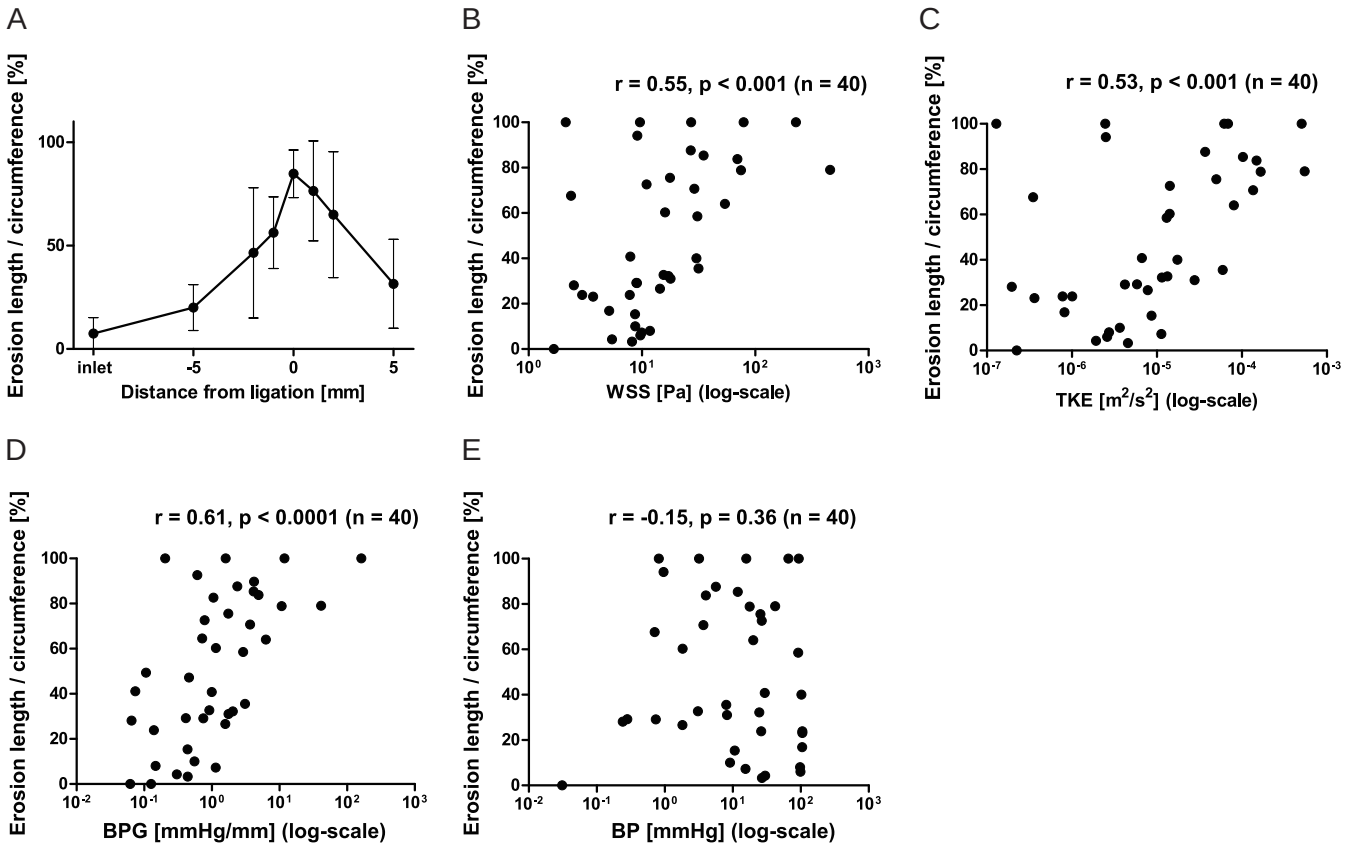

Fig. 3. Relationship between the extent of erosive injury and WSS, TKE, BPG and BP.

The ratio of the length of erosive injury to the luminal circumference was measured in the histological sections. A. Extent of erosive injury at a longitudinal distance from the stenotic portion ($n=5$). B-E. Relationships between the extent of erosive injury and WSS (B), TKE (C), BPG (D) and BP (E) (two-tailed Spearman's rank correlation test).

of acute cardiovascular events that is characterized by superficial erosive injury of SMC-rich plaque[5]. Acute luminal changes due to vasoconstriction or stenosis can induce erosive injury in areas of SMC-rich atherosclerotic plaque[12, 14]; however, the underlying hemodynamic factors remain unknown. The WSS is a parameter of force that directly acts tangentially on the vascular luminal surface. The TKE is a parameter of the local strength of turbulence and represents the divergence of the flow velocity. The notion has been established that a steady laminar flow plays a protective role with respect to the endothelial function and survival, whereas a disturbed flow has an adverse effect on endothelial cells[12, 21, 22]. Therefore, the increase in WSS and/or TKE is likely to induce erosive injury in areas of SMC-rich plaque.

A turbulent flow can induce morphological changes and the detachment of arterial endothelial cells. Fry[13] reported that turbulent shear stress induced by acute aortic stenosis promotes changes in endothelial shape and detachment at the post-stenotic portion in a canine model of the normal aorta. The calculated value of acute yield stress at the portion was $>37.9 \pm 8.5$ Pa. The value of WSS at the erosive injury portion in our model was approximately 50% lower. Meanwhile, Kolodgie *et al.*[23] proposed that the extracellular matrix at sites of SMC-rich plaque interferes with the integrity of the endothelium. Although the vascular size in Fry's and the present model differed, the matrix components of SMC-rich plaques may affect plaque fragility. On the other hand, Campbell *et al.*[24] recently generated patient-specific 3D-models of the coronary arteries from biplane angiographic images of three patients with plaque erosion and found that neither a high nor low magnitude of mean WSS is associated with sites of plaque erosion and that the oscillatory shear index and local curvature are not associated with erosion *per se*. We are unable to explain this discrepancy; however, the angiograms of the patients evaluated in their study were acquired after thrombectomy,

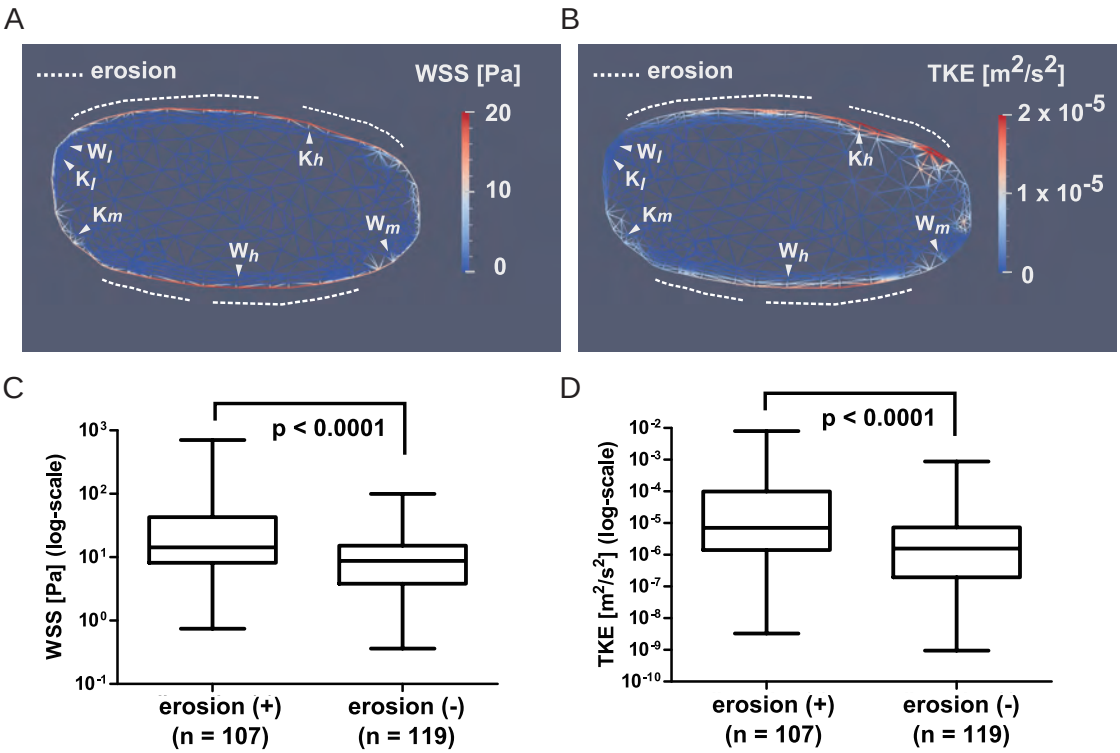

Fig. 4. Values for WSS and TKE at points with and without erosive injury.

Representative cross sectional images of WSS (A) and TKE (B) 2 mm distal from the most stenotic portion. The dotted lines indicate sites of erosive injury. The values for WSS and TKE are similar but unevenly distributed in the area of plaque. The sites of erosive injury tend to localize at areas of higher WSS and TKE values (W_h, highest WSS; K_h, highest TKE; W_m, median WSS; K_m, median TKE; W_l, lowest WSS; K_l, lowest TKE).
The magnitudes of WSS (C) and TKE (D) are significantly higher at points with, compared to without, erosive injury (two-tailed Mann-Whitney *U*-test).

and morphological changes following intervention therapy may affect outcomes.

Blood pressure and BPG are important factors involved in inducing endothelial cell injury. Svendsen *et al.*[9] reported a significant association between an elevated BP and endothelial cell injury in a rabbit model of renal artery stenosis. In addition, Li *et al.*[25] examined the effects of WSS and BPG on plaque disruption under a pulsatile viscous flow using a rigid tube with asymmetric stenosis and concluded that BPG was more powerful than WSS in terms of inducing plaque injury. These results indicate that BP and BPG are significant factors involved in damage to areas of atherosclerotic plaque. We found that BPG closely correlated with erosive injury, whereas BP did not. The BPG accelerates the flow velocity, which increases the WSS and TKE and may exert vertical torsion on the endothelium. These processes can be considered to induce erosive injury.

The magnitude of TKE was also higher at the eroded than at the non-eroded points. Magnetic resonance imaging (MRI) now allows for the non-invasive estimation of TKE *in vivo*[26, 27]. Lantz *et al.* assessed TKE values using MRI in a patient with aortic coarctation before and after catheter intervention[26] and concluded that MRI-based TKE measurements are useful for evaluating intervention outcomes. In addition, Dyverfeldt *et al.* closely correlated the MRI values of TKE with irreversible pressure loss measured on echocardiography in 14 patients with aortic stenosis[27]. The measurement of TKE using MRI is therefore a novel tool for the non-invasive diagnosis of plaque erosion.

Human pathological studies have documented plaque erosion in the cerebral and carotid arteries as well as coronary arteries[28, 29], while clinical studies have reported vasoconstriction and/or vasospasm of the cerebral arteries to be associated with cerebral thrombosis[30, 31]. However, the contribution of hemodynamic changes induced by vasoconstriction to erosive injury in these arteries remains unknown. Further investigation is thus required to clarify this issue.

This study is associated with several limitations. The elasticity of the vascular wall was not taken into account, which would decrease the WSS, TKE and BPG values. In addition, the pulsatile flow may have had some effects on the incidence of erosive injury in our model. However, we were unable to obtain a valid pulsatile flow pattern applicable for CFD simulation because the vessel size was small and the blood flow was highly reduced. Further studies of the case-specific nature of a pulsatile flow would help to clarify these effects.

Conclusion

In this study, we discovered that increased WSS, TKE and BPG values closely correlate with the development of erosion in areas of SMC-rich plaque in a rabbit model of SMC-rich atherosclerotic plaque *in vivo*. This mechanism may be involved in plaque erosion in atherosclerotic human coronary arteries.

Acknowledgements

The study was supported in part by Grants-in-Aid for Scientific Research in Japan (Nos. 25560205 N.S., 23790410, 25460440 A.Y., 23390084 Y.A.), the Mitsubishi Pharma Research Foundation (A.Y.) and the Integrated Research Project for Human and Veterinary Medicine, University of Miyazaki (A.Y., Y.A.).

Conflicts of Interest

None.

References

1) Falk E, Nakano M, Bentzon JF, Finn AV, Virmani R: Update on acute coronary syndromes: the pathologists' view. Eur Heart J, 2013; 34: 719-728
2) Libby P: Mechanisms of acute coronary syndromes and their implications for therapy. N Engl J Med, 2013; 368: 2004-2013
3) Mizuno Y, Jacob RF, Mason RP: Inflammation and the development of atherosclerosis. J Atheroscler Thromb, 2011; 18: 351-358
4) Sato Y, Hatakeyama K, Yamashita A, Marutsuka K, Sumiyoshi A, Asada Y: Proportion of fibrin and platelets differs in thrombi on ruptured and eroded coronary atherosclerotic plaques in humans. Heart, 2005; 91: 526-530
5) Farb A, Burke AP, Tang AL, Liang TY, Mannan P, Smialek J, Virmani R: Coronary plaque erosion without rupture into a lipid core. A frequent cause of coronary thrombosis in sudden coronary death. Circulation, 1996; 93: 1354-1363
6) Burke AP, Farb A, Malcom GT, Liang YH, Smialek J, Virmani R: Coronary risk factors and plaque morphology in men with coronary disease who died suddenly. N Engl J Med, 1997; 336: 1276-1282
7) Arbustini E, Dal Bello B, Morbini P, Burke AP, Bocciarelli M, Specchia G, Virmani R: Plaque erosion is a major substrate for coronary thrombosis in acute myocardial infarction. Heart, 1999; 82: 269-272
8) Fukumoto Y, Hiro T, Fujii T, Hashimoto G, Fujimura T, Yamada J, Okamura T, Matsuzaki M: Localized elevation of shear stress is related to coronary plaque rupture: a 3-dimensional intravascular ultrasound study with in-vivo color mapping of shear stress distribution. J Am Coll Cardiol, 2008; 51: 645-650
9) Svendsen E, Tindall AR: Raised blood pressure and endothelial cell injury in rabbit aorta. Acta Pathol Microbiol Scand A, 1981; 89: 325-334
10) Muller JE, Tofler GH, Stone PH: Circadian variation and triggers of onset of acute cardiovascular disease. Circulation, 1989; 79: 733-743
11) Cheng GC, Loree HM, Kamm RD, Fishbein MC, Lee RT: Distribution of circumferential stress in ruptured and stable atherosclerotic lesions. A structural analysis with histopathological correlation. Circulation, 1993; 87: 1179-1187
12) Tricot O, Mallat Z, Heymes C, Belmin J, Leseche G, Tedgui A: Relation between endothelial cell apoptosis and blood flow direction in human atherosclerotic plaques. Circulation, 2000; 101: 2450-2453
13) Fry DL: Acute vascular endothelial changes associated with increased blood velocity gradients. Circ Res, 1968; 22: 165-197
14) Gertz SD, Uretsky G, Wajnberg RS, Navot N, Gotsman MS: Endothelial cell damage and thrombus formation after partial arterial constriction: relevance to the role of coronary artery spasm in the pathogenesis of myocardial infarction. Circulation, 1981; 63: 476-486
15) Sumi T, Yamashita A, Matsuda S, Goto S, Nishihira K, Furukoji E, Sugimura H, Kawahara H, Imamura T, Kitamura K, Tamura S, Asada Y: Disturbed blood flow induces erosive injury to smooth muscle cell-rich neointima and promotes thrombus formation in rabbit femoral arteries. J Thromb Haemost, 2010; 8: 1394-1402
16) Brill A, Fuchs TA, Chauhan AK, Yang JJ, De Meyer SF, Köllnberger M, Wakefield TW, Lämmle B, Massberg S, Wagner DD: von Willebrand factor-mediated platelet adhesion is critical for deep vein thrombosis in mouse models. Blood, 2011; 117: 1400-1407
17) Yamashita A, Furukoji E, Marutsuka K, Hatakeyama K, Yamamoto H, Tamura S, Ikeda Y, Sumiyoshi A, Asada Y: Increased vascular wall thrombogenicity combined with reduced blood flow promotes occlusive thrombus formation in rabbit femoral artery. Arterioscler Thromb Vasc Biol, 2004; 24: 2420-2424
18) Windberger U, Bartholovitsch A, Plasenzotti R, Korak KJ, Heinze G: Whole blood viscosity, plasma viscosity and erythrocyte aggregation in nine mammalian species: reference values and comparison of data. Exp Physiol, 2003; 88: 4331-4440
19) Kenner T, Leopold H, Hinghofer-Szalkay H: The continuous high-precision measurement of the density of flow-

ing blood. Pflugers Arch, 1977; 370: 25-29
20) Ferziger JH, Peric M: Computational Methods for Fluid Dynamics. Springer, Heidelberg, Germany, 2002
21) Jeon H, Boo YC: Laminar shear stress enhances endothelial cell survival through a NADPH oxidase 2-dependent mechanism. Biochem Biophys Res Commun, 2013; 430: 460-465
22) Resnick N, Yahav H, Shay-Salit A, Shushy M, Schubert S, Zilberman LCM, Wofovitz E: Fluid shear stress and the vascular endothelium: for better and for worse. Prog Biophys Mol Biol, 2003; 81: 177-199
23) Kolodgie FD, Burke AP, Farb A, Weber DK, Kutys R, Wight TN, Virmani R: Differential accumulation of proteoglycans and hyaluronan in culprit lesions: insights into plaque erosion. Arterioscler Thromb Vasc Biol, 2002; 22: 1642-1648
24) Campbell IC, Timmins LH, Giddens DP, Virmani R, Veneziani A, Rab ST, Samady H, McDaniel MC, Finn AV, Taylor WR, Oshinski JN: Computational Fluid Dynamics Simulations of Hemodynamics in Plaque Erosion. Cardiovasc Eng Technol, 2013; 4: doi: 10.1007/s13239-013-0165-3
25) Li ZY, Taviani V, Tang T, Sadat U, Young V, Patterson A, Graves M, Gillard JH: The mechanical triggers of plaque rupture: shear stress vs pressure gradient. Br J Radiol, 2009; 82 Spec No 1: S39-45
26) Lantz J, Ebbers T, Engvall J, Karlsson M: Numerical and experimental assessment of turbulent kinetic energy in an aortic coarctation. J Biomech, 2013; 46: 1851-1858
27) Dyverfeldt P, Hope MD, Tseng EE, Saloner D: Magnetic resonance measurement of turbulent kinetic energy for the estimation of irreversible pressure loss in aortic stenosis. JACC Cardiovasc Imaging, 2013; 6: 64-71
28) Ogata J, Yutani C, Otsubo R, Yamanishi H, Naritomi H, Yamaguchi T, Minematsu K: Heart and vessel pathology underlying brain infarction in 142 stroke patients. Ann Neurol, 2008; 63: 770-781
29) Spagnoli LG, Mauriello A, Sangiorgi G, Fratoni S, Bonanno E, Schwartz RS, Piepgras DG, Pistolese R, Ippoliti A, Holmes DR Jr: Extracranial thrombotically active carotid plaque as a risk factor for ischemic stroke. JAMA, 2004; 292: 1845-1852
30) Ducros A, Boukobza M, Porcher R, Sarov M, Valade D, Bousser MG: The clinical and radiological spectrum of reversible cerebral vasoconstriction syndrome. A prospectiveseries of 67 patients. Brain, 2007; 130: 3091-3101
31) Konzen JP, Levine SR, Garcia JH: Vasospasm and thrombus formation as possible mechanisms of stroke related to alkaloidal cocaine. Stroke, 1995; 26: 1114-1118